Developing high resolution water balance estimates of tailings storage facilities

Jason Keller
GeoSystems Analysis, Inc., Hood River, OR, USA

Michael Milczarek
GeoSystems Analysis, Inc., Tucson, AZ, USA

Michael Geddis
KGHM International, Tucson, AZ, USA

ABSTRACT: A comprehensive tailings storage facility (TSF) water balance study was conducted to estimate seepage rates during past operations and under proposed future TSF expansion. Multiple methods were used to achieve these objectives: 1) Daily estimates of operational water inflows and outflows were prepared to include high resolution estimates of monthly evaporation rates using Landsat satellite imagery and an energy balance model; 2) A characterization program was conducted to measure tailings *in situ* and laboratory physical and hydraulic properties; 3) These measurements were used to classify the tailings into different material types that correlated to distance from the main cycloned embankment and TSF perimeter; 4) Operational data and satellite imagery were analyzed to estimate the TSF area and supernatant ponded area over time; 5) A TSF hydraulic property model was developed to spatially distribute the different material types within the TSF over time and assign hydraulic properties from the surface to depth. Water balance results indicate that seepage rates are decreasing over time due to operational improvements and reduced tailings permeability due to consolidation at depth. The TSF hydraulic property model indicates that seepage rates are highest along the perimeter of the TSF below ponded areas.

1 INTRODUCTION

Tailings storage facilities (TSFs) are large, often being more than 500 hectares in size, and of variable thickness, ranging from less than one meter near the perimeter to significant depths at the impoundment dam and in the interior. TSF construction methods create multiple and variable layers of distinct tailings textures due to alternating methods and periods of tailings deposition (e.g., slurry in the winter, cyclone in the summer) and movement of tailings deposition sources, both slurry points and moving banks of cyclones. Additionally, tailings consolidation due to settling and over-burden pressure results in long-term physical and hydraulic property changes due to compaction at depth. Consequently, water balance estimates of tailings storage, supernatant evaporation and seepage rates are confounded by the large spatial and temporal depositional variations across a TSF due to construction and operational practices and climatic conditions.

A comprehensive water balance study was conducted to develop hydraulic property and water balance models to quantify past and future (expanded) seepage rates from an unlined TSF and estimate uncertainty. Multiple methods were used to achieve these objectives including detailed estimates of water inflows and outflows, *in situ* and laboratory measurements of the tailings physical and hydraulic properties, analysis of operations data and satellite imagery to estimate the TSF supernatant and tailings depositional spread, and classification and delineation of tailings into different material types. A hydraulic property model was developed based on the field and laboratory data and was then used to predict the spatial distribution of seepage across the TSF. The water balance results were used to guide TSF expansion design and water manage-

ment to reduce TSF seepage, and as the upper boundary condition for a fate and transport groundwater flow model.

1.1 *Tailings Storage Facility Overview*

The TSF is in a semi-arid, cold desert, climate with an average December temperature (coldest month) of -4 °C and an average July temperature (warmest month) of 20 °C. The tailings embankment is constructed using centerline raise methods with cyclone underflow sand deposition. Cyclone deposition typically occurs during the summer (May to September) with whole tailings deposition via spigotting from various locations on the perimeter of the facility from October to April. The TSF began operating in January 1996. Mining operations were suspended between July 1999 and September 2004. Tailings deposition resumed October 2004 with the restart of mining operation. The TSF was approximately 670 hectares in 2020.

Supernatant is reclaimed from the TSF at the barge operating channel (BOC, Figure 1). The BOC consists of bentonite-amended and compacted alluvium. Recently, the BOC area was enclosed with a ring-road/dyke, and shore-based pumps have been used to maintain the water level at the lowest possible operational depth, all to reduce seepage from the BOC. Future expansion of the BOC includes installation of a HDPE liner under an expansion area, and then intentionally breaching the ring-road to create a lined BOC with minimal seepage. Water is pumped from the BOC to the Repulp building (Figure 1) and either recirculated to bring tailings up to the optimal percent solids required for cyclone operation or sent back to the mill as reclaim water.

1.2 *Conceptual Model of Hydrologic Conditions*

Because tailings emplacement is a fluvial depositional process, the largest tailing particles settle nearest to the cyclone or spigot, whereas finer-grained tailings settle farther away from the deposition source. This process results in tailings segregation into material "types" with different physical and hydraulic properties that determine the amount of water the tailings will retain and lose to seepage. The cycloned main embankment (CME) is constructed from coarse-grained underflow, and the overflow is sent either past the cyclones, or out into the impoundment about 100 feet to form the upstream beach area. The coarse-grained sand in the CME has much higher permeability than the fine-grained overflow of the beach. Moderate permeability tailings represent a transition between coarse-grained tailings to low permeability fine-grained tailings as the slurry moves from the depositional source to the BOC. In addition to the areal distribution of tailings types, the tailing permeability tends to decrease with depth in the TSF as increasing overburden pressure results in tailings compaction.

The tailings surface consists of zones of wet tailings and shallow surficial channels with a large, ponded area between the CME beach and the BOC. Evaporation occurs from these wet areas and to a lesser extent from tailings that are drying between deposition cycles. Evaporation varies significantly between summer and winter, as do depositional practices, both of which control seepage rates. Consequently, seepage from the TSF is expected to be variable through time and space as a function of tailings deposition and growth rates, cyclone sand production, presence of ponded and wet tailings outside of the BOC, evaporative losses and residual pore water that is not lost to evaporation. However, the variability in seepage rates likely reduces with depth through the tailings, primarily because of decreasing permeability with depth, resulting in nearly constant net percolation from the base of the facility. This net percolation is reduced by reclaiming more water and limiting the spatial extent of deposition, both of which have been accomplished over the past several years.

2 METHODS

2.1 *Field Characterization Program*

The field characterization program consisted of:

- Three auger hole transects to log tailings geology and physical attributes (texture and color) and to evaluate layering and segregation;
- *in situ* measurement of seepage within the BOC using a seepage meter;
- *in situ* measurement of tailings saturated hydraulic conductivity (K_{sat});
- *in situ* measurement of K_{sat} of alluvial sediments that represent alluvium under the TSF, and;
- collection of tailings and alluvium samples for laboratory physical and hydraulic testing.

Locations evaluated as part of the field characterization program are shown in Figure 1 and consist of points where auger holes were advanced to collect samples for geologic logging and laboratory testing, and/or *in situ* (field) hydraulic testing.

In situ hydraulic property testing was conducted using a variety of methods to directly measure seepage fluxes within tailings and BOC areas under ponded conditions, or to estimate *in situ* K_{sat} of tailings and alluvium material. Testing was completed using either single-ring cylinder infiltrometer (CI) (Bouwer et al., 1999), air-entry permeameter (Bouwer, 1966), Wooding's infiltrometer (Wooding, 1968), tension infiltrometer (Hussen and Warrick, 1993), or seepage meter (Lee, 1977) measurements. Additionally, CI measurements were made in areas where shallow water conditions prevented the use of the traditional seepage meter method.
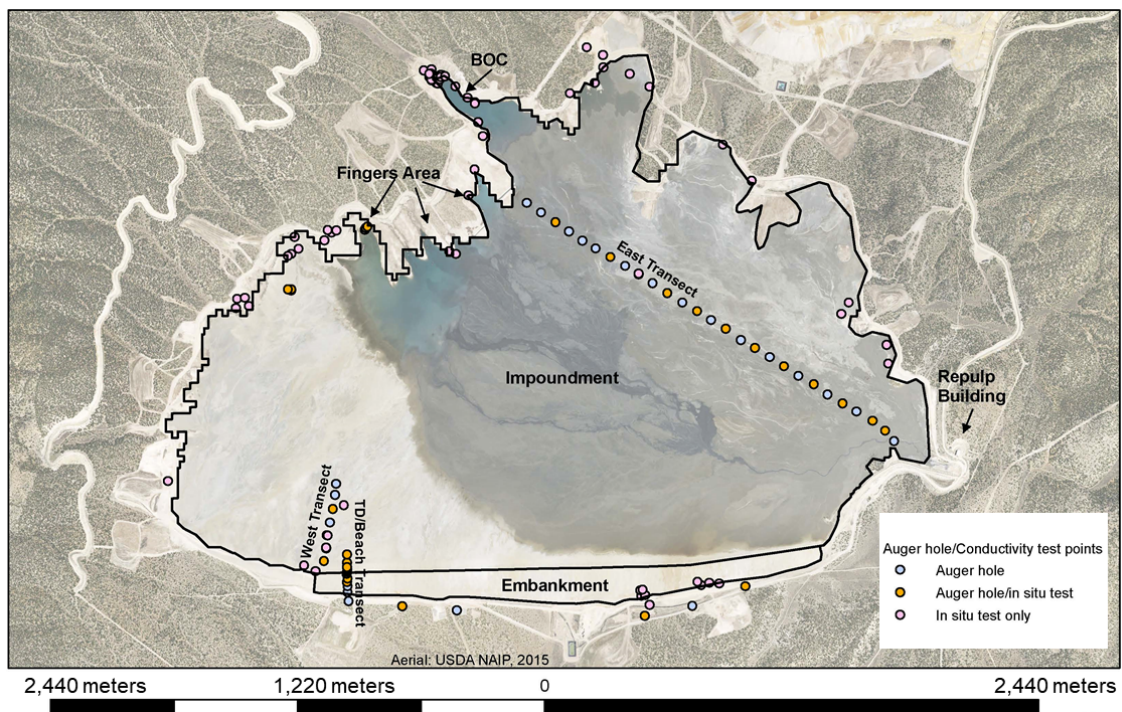

Figure 1. Near surface investigation locations.

2.2 *Laboratory Testing*

A subset of tailings samples collected during the field investigation were selected for laboratory physical and hydraulic property testing, to include particle size distribution (PSD), particle density, 1-D consolidation, K_{sat}, triaxial permeability and moisture retention characteristics (MRC). Twenty (20) samples representing the range of observed tailings field textures were selected and analyzed for PSD and particle density to allow for laboratory calibration of the 221 field texture estimates. Seven composite tailings samples were created for 1-D consolidation, K_{sat} and MRC testing based on the estimated distribution of tailing types from field texture measurements. Three of the seven composite tailings samples were also selected for triaxial permeability testing. Each composite tailings sample was created from two grab samples with similar texture.

Tailings dry bulk densities as a function of depth were estimated from the 1-D consolidation and triaxial permeability testing results, which were used to guide the target remolded dry bulk densities (BD) for the K_{sat} and MRC tests. K_{sat} and MRC tests were conducted in 2-inch diameter columns remolded to high and low dry BDs representative of tailings conditions under greater than 45 m of depth, and between 0 and 45 m of depth respectively.

2.3 Area and Thickness Estimates

The boundary of the TSF between 1996 and 2020 was estimated on an approximate six-month time interval using Landsat and Sentinel satellite data and application of a site-specific processing algorithm. The estimated TSF ponded and dry areas were validated against aerial photographs and estimated TSF area reported in mine annual monitoring reports. Linear interpolation of the delineated TSF areas generated a monthly time series of ponded, dry, and partially saturated TSF surface areas. The boundary between the TSF embankment and impoundment area was based on the static location of the cyclone header pipe visible in aerial photographs. TSF material thicknesses were estimated annually (1996 to 2020) as the difference between the pre-mining and TSF surface topography.

2.4 Water Balance Estimates

The water balance components of the TSF incorporated into the water balance model are shown in Figure 2. The methods used to calculate or estimate flux rates for the various components are described below.
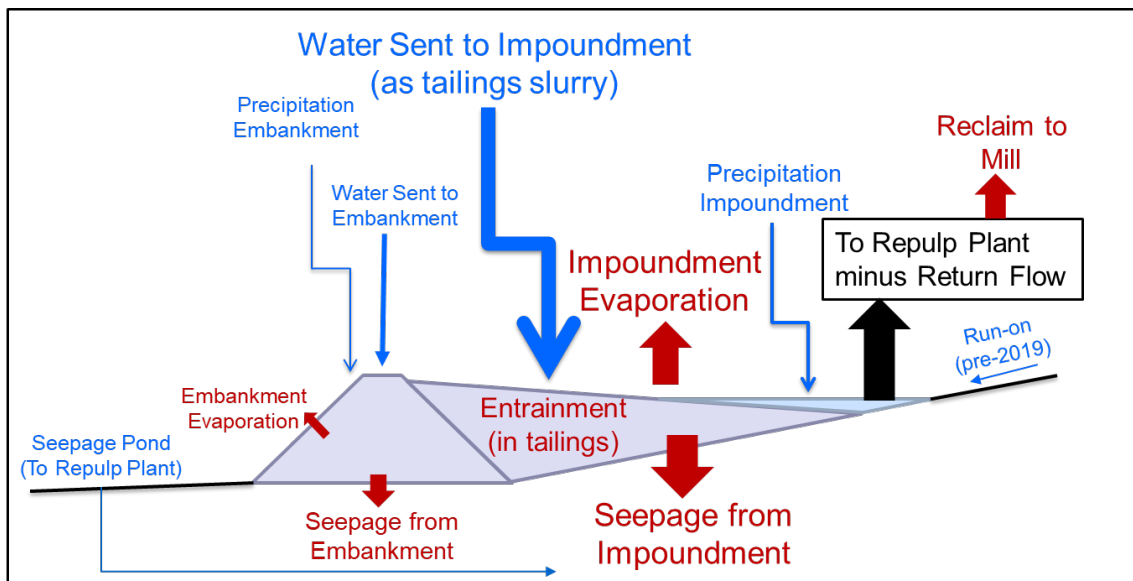

Figure 2. TSF water balance.

2.4.1 Inflow

− Tailings Slurry: Two (2) thickeners at the Mill each produce an underflow of condensed tailings slurry that is sent to the TSF. The percentage of solids is estimated using a nuclear transmission style density gauge. By assuming a grain density of 2.7 g/cm^3, the amount of water in the slurry is obtained by difference. Daily estimates of the quantity of water within the tailings slurry was partitioned into water sent to the impoundment and water deposited at the CME. Tailings water flow rates into the CME were dependent on the solids density of the cyclone underflow and the cyclone split between overflow and underflow.
− Precipitation: Daily measured precipitation values from a meteorological station located adjacent to the TSF embankment were applied to the embankment and the impoundment using the TSF area delineations from the satellite imagery.

- Run-on: Daily run-on into the TSF was estimated from the daily precipitation values using the Soil Conservation Service (SCS) curve number (CN) method (USDA, 1986) and the contributing catchment area (which decreased monthly as the TSF area increased). A CN value of 76 was applied, consistent with the value used for the TSF design. Run-on was assumed to be zero due to construction of an alluvium embankment around the west, north, and east perimeter of the TSF in January of 2019.

2.4.2 *Outflow*

- Reclaim water: Daily reclaim water rates were based on measured flow rates from the TSF to the mill. In February 2018 the TSF water reclaim volume increased with the installation of shore-based suction pumps at the BOC. The pump intakes can keep the BOC water level lower than the old barge set-up, thereby decreasing the amount of water left at the BOC, which reduces water available for net percolation.
- Evaporation: Daily evaporation rates were estimated using the three-temperature (3T) energy balance model (Qiu and Zhao, 2010) from local weather data and Landsat 7 and 8 satellite imagery. A summary of the 3T model methodology is provided in Keller et al. (2018).
- Tailing water entrainment: The initial amount of water entrained within the tailings pore space is a function of the slurry flow rate and density of contained solids, the tailings MRCs, and dry BD. The MRC and dry BD for each of the different tailing types were calculated using the conceptual tailings type distribution model, and their estimated distribution over time (Section 3.4). High to moderate permeability tailings associated with the embankment and beach areas were assumed to drain to field capacity after placement, while moderate to low permeability tailings associated with the impoundment were assumed to remain saturated.
- Seepage: Monthly seepage was determined by the difference between total monthly inflow minus outflow from the impoundment and embankment areas separately. Predicted seepage rates calculated from the water balance represent an instantaneous value; in reality, changes in water fluxes are attenuated within the TSF and result in a nearly continuous average TSF seepage with some variability driven by changes along the perimeter during operations.

2.5 *Distributed Seepage*

Estimated seepage from across the TSF was distributed based on the hydraulic property model for the TSF (See also Section 3.4):
- tailings material type and thickness classification and associated K_{sat} values;
- measured seepage fluxes for ponded tailings, and;
- distribution of ponded areas as determined from satellite imagery.

The TSF was divided into 30 m by 30 m rectangular grid cells coincident with the Landsat satellite imagery dataset. Embankment seepage rates were calculated within the water balance model and distributed uniformly across the embankment. The estimated seepage from the unlined BOC was based on the mean seepage flux measured within the BOC side slopes and floor (Section 3.1). Estimated seepage rates from the future HDPE lined BOC areas are assumed to be negligible ($< 1x10^{-9}$ cm/s, Giroud and Bonaparte, 1989). Lined and unlined BOC seepage were applied directly and subtracted from the water balance calculated impoundment seepage.

For tailing areas not within the BOC, seepage rates were calculated for each grid cell depending on the tailings type and thickness at each cell. Seepage rates were assumed to be equivalent to the K_{sat}, determined for each tailings type, as modified by the tailing thickness ranges (<15 m, 15 to 45 m, and >45 m) present at each cell. If the tailings thickness was less than 15 m in a cell under surface ponding as determined from the 3T energy balance model, the estimated seepage used the geometric mean of *in situ* measured K_{sat} values from ponded areas outside of the BOC (Section 3.1). For each month, the water balance model calculated seepage was distributed across each grid cell based on the assigned grid cell estimated seepage (i.e., K_{sat}).

Spatially distributed maps of calculated seepage throughout the impoundment and embankment were created semiannually using the average of the six-month period encompassing the months October through March and April through September. The semiannual period approximates months without (October through March) and with (April through September) cycloning.

3 RESULTS

3.1 *TSF Field Characterization*

Tailing materials to depths of 3 m within the TSF East and West transects were composed of alternating layers of sandy and finer-grained tailings caused by the annual change from cycloning to spigotting deposition methods. Tailing percent fines (<0.075 mm) material profiles are shown for the East transect (Figure 3) and the West transect (Figure 4). At the East transect, the predominance of layering and percent fines increased with distance from the spigot and cyclones deposition sources from approximately 30-60% fines within 800 m of the deposition sources to 50-70% fines at distances greater than 800 m. The observed increase in layers with a higher percent fines represents the depositional segregation of tailings from the east side of the TSF towards the BOC. Observed finer over coarser grained layers represents cyclone overflow tailings that were deposited during the summer months on top of slurry tailings. On the West transect, tailings less than 30 m from the CME centerline were consistently sandy (<30% fines) throughout the profile. Immediately downstream of this sandy beach zone, the percentage of fines significantly increased (50 to 70% fines), reflecting the transition from cyclone underflow to cyclone overflow tailings.
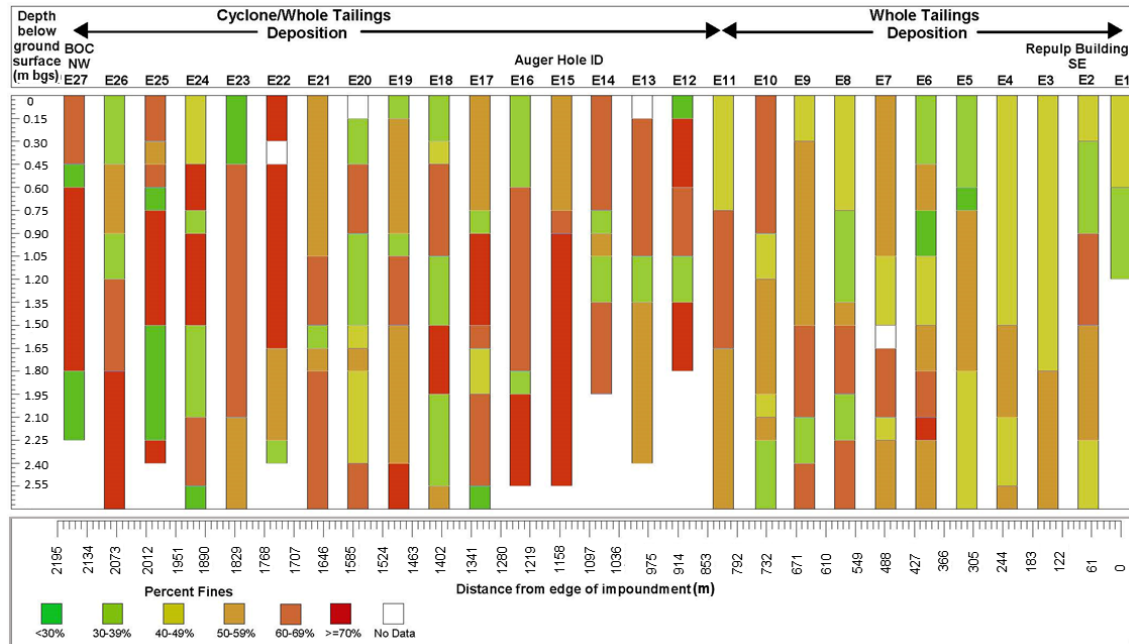

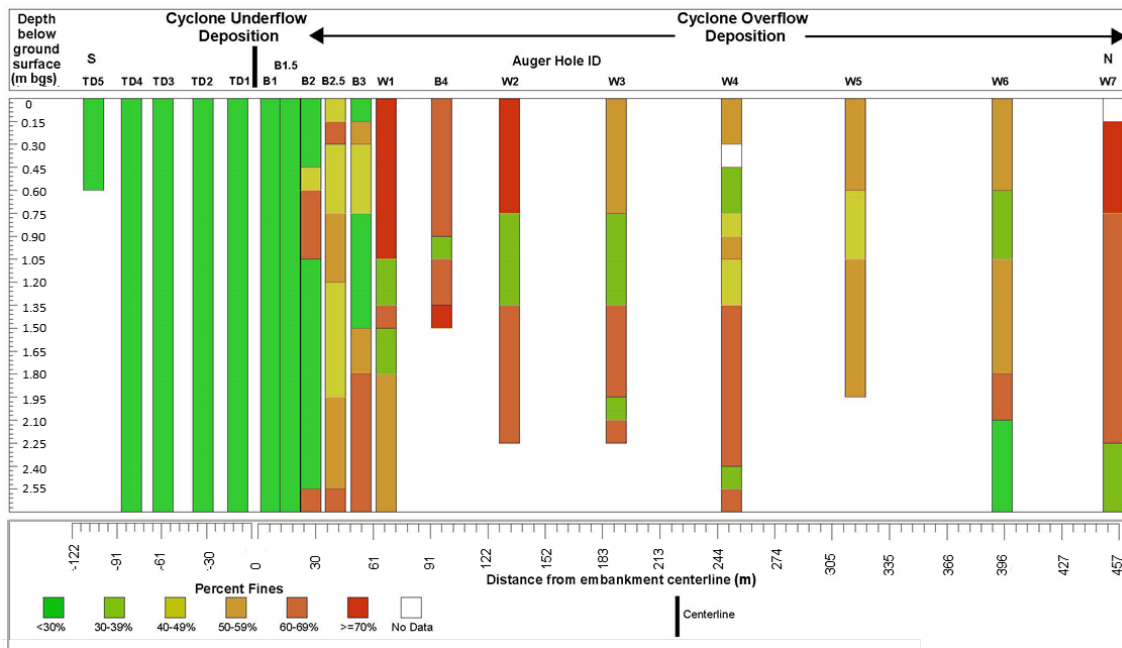Figure 3. East transect percent fines profile.

Figure 4. Embankment-beach-west transect percent fines profile.

Results of the tailings *in situ* K_{sat} tests (Woodings (n=21), air entry permeameter (n=7), tension infiltrometer (n=2)) are plotted in Figure 5 as a function of the percent fines. Measured K_{sat} values ranged from between 3.7×10^{-3} centimeters per second (cm/s) to 3.8×10^{-6} cm/s and decreased exponentially as a function of increasing fines content. The geometric mean K_{sat} value ranged from 2.1×10^{-3} cm/s for <30% fines to 1.9×10^{-5} cm/s for >70% fines.

Seepage meter tests completed on the floor of the BOC (constant head and CI, n=4) measured K_{sat} values between 9.3×10^{-6} cm/s to 3.8×10^{-6} cm/s with a geometric mean of 5.7×10^{-6} cm/s. CI tests on the BOC side slopes (n=8) indicated higher flux rates with a range between 8.5×10^{-5} cm/s to 1.5×10^{-5} cm/s and a geometric mean of 3.5×10^{-5} cm/s. Increased seepage along the BOC side slopes may represent variability in bentonite amendment permeability reductions. Arial images were analyzed to estimate the fraction of the BOC between the floor (80%) and side slope (20%). This estimated ratio of side slope to floor was used to calculate a weighted flux rate for the BOC equal to 1.2×10^{-5} cm/s.
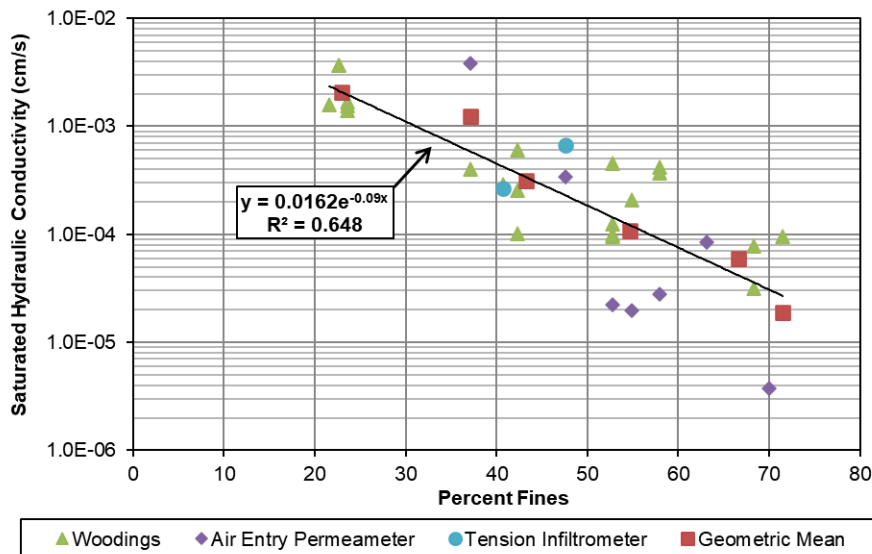

Figure 5. Tailings percent fines as a function of field measured saturated hydraulic conductivity.

3.2 *Laboratory Testing*

Rigid wall and triaxial flex-wall K_{sat} testing was conducted at different bulk densities, equivalent to tailings depths ranging from 23, 45 and 76 m bgs. *In situ* K_{sat} testing results were used to estimate the tailing material types K_{sat} as a function of tailings depth (Figure 6).
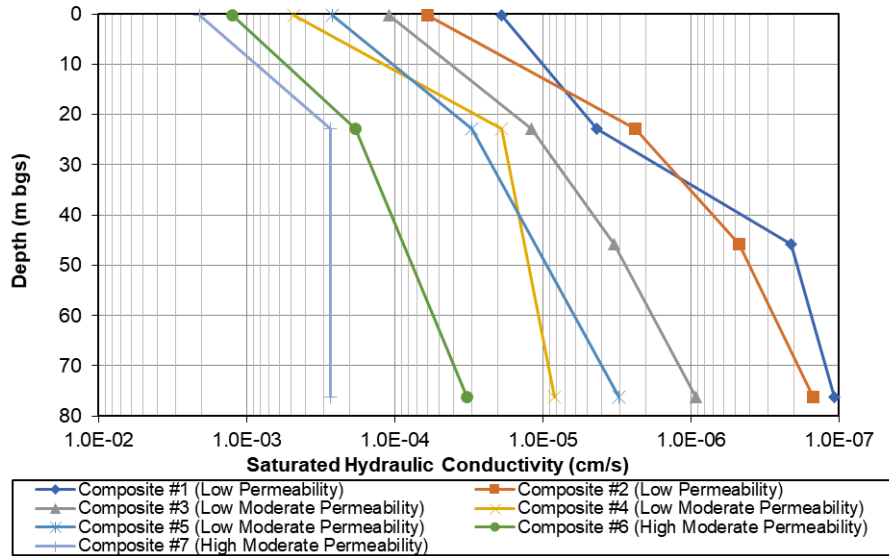

Figure 6. Saturated hydraulic conductivity as a function of tailings depth.

The data indicate that lower percent fine contents correlate with higher K_{sat} values that decrease nonlinearly as tailings depth increases. Comparable K_{sat} values measured between different composite samples allowed representative permeability classifications of Low, Moderate, and High Permeability Tailings to be developed (Figure 6).

3.3 *TSF Boundary and Thickness*

The TSF boundary delineation and thickness evaluation is shown for selected timeframes during operations in Figure 7. The satellite estimated TSF areas were in good agreement with the estimated areas calculated by the mine. The TSF showed a rapid growth progression between 1996 and 1999 during early operations. After the temporary shutdown (1999-2004), tailings growth between 2004 and 2015 primarily occurred along the northern and western edges of the facility. The estimated TSF growth from 2021 through 2028 will occur mainly in the vertical direction. For example, the TSF area in 2018 (approximately 650 hectares) will increase by approximately 50 hectares before closure in 2028 (700 hectares acres total); and the thickness of tailings will increase by approximately 15 m.
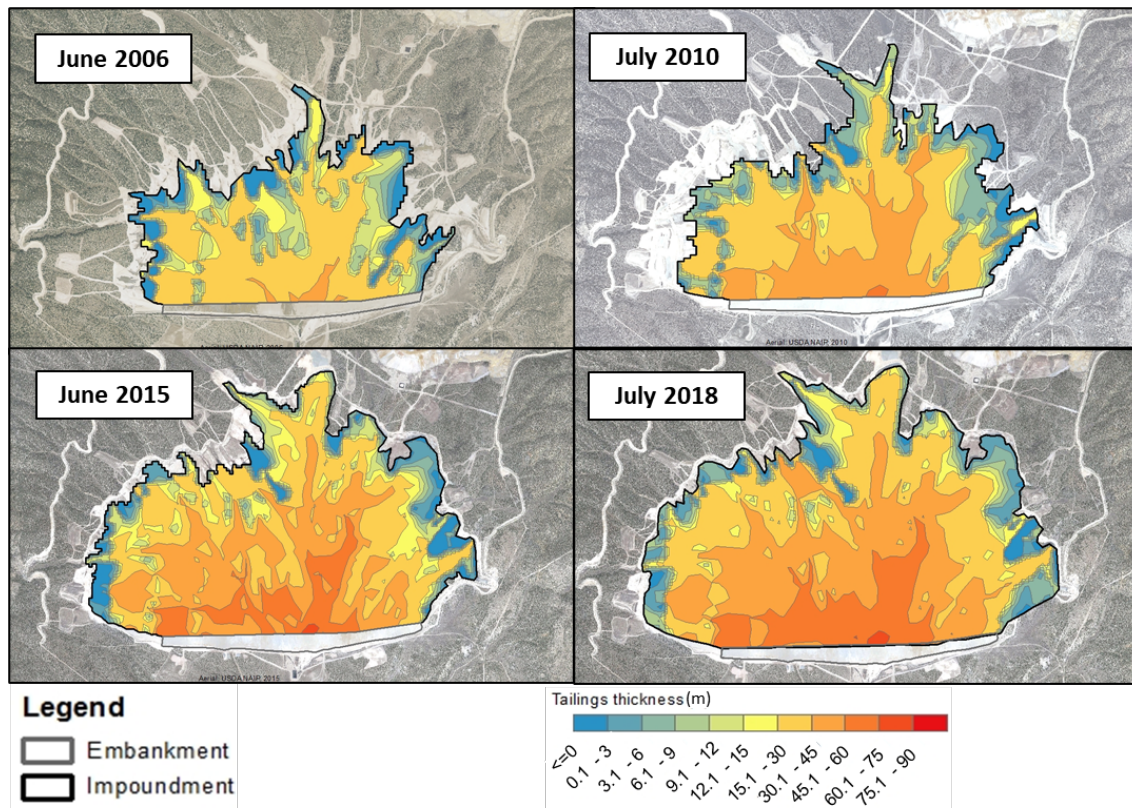
Figure 7. TSF boundary and thickness at select time periods.

3.4 *TSF Hydraulic Property Model*

The measured physical and hydraulic properties can be classified into Low, Moderate, and High Permeability tailings based on their location with respect to distance from the tailings deposition source. K_{sat} assignments for these material types as a function of tailings thickness were estimated from the depth-permeability curves (Figure 6) and are summarized in Table 1.

The tailings permeability type classification, geologic log transect data, and consideration of surface flow paths and fluvial deposition processes were used to estimate the growth and spatial distribution of tailings material types each month. Aerial and vertical representations of the tailings material types for select timeframes during operations are shown in Figure 8.

Table 1. Tailings material type, thickness, and hydraulic conductivity assigned to distribute seepage

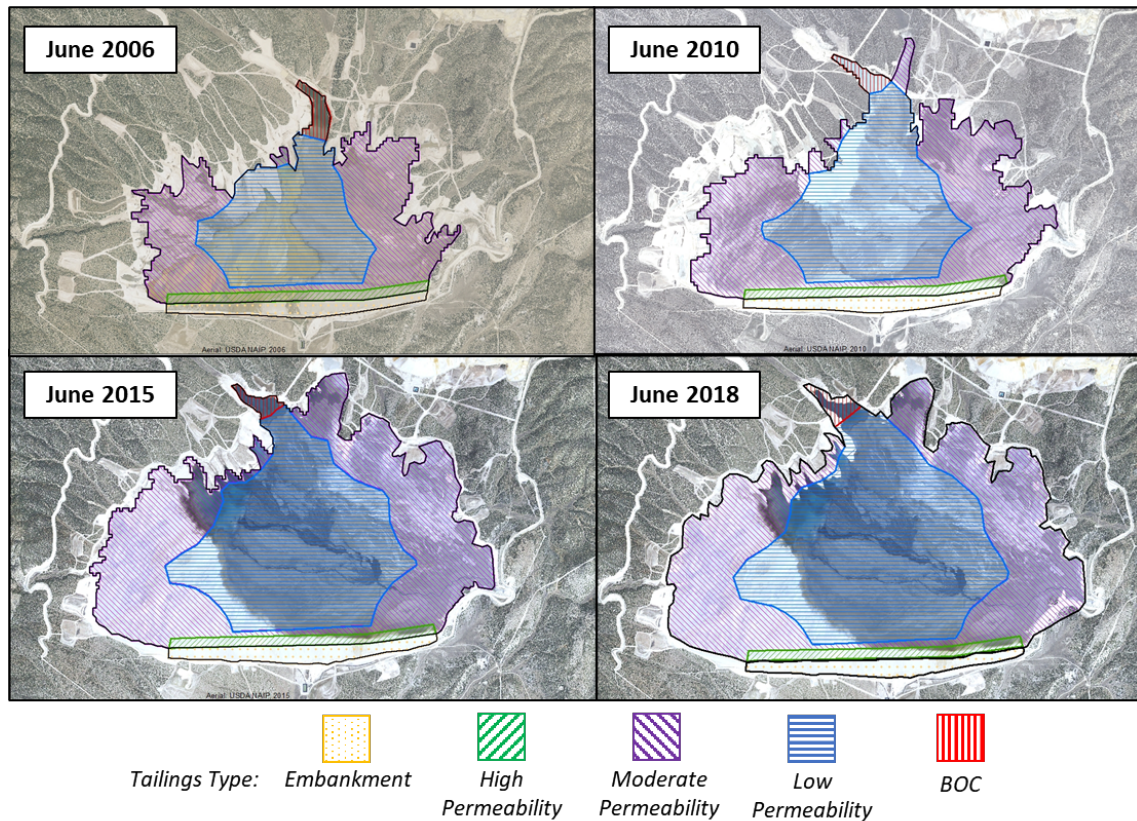| Tailings Material Type	Tailings Thickness (m)	Hydraulic Conductivity (cm/s)
Unlined Ponded BOC	-	1.20E-05
Lined Ponded BOC	-	1.00E-09
Ponded Tailings	<3	6.50E-05
High Permeability Tailings	<15	1.80E-05
	15 - 45	7.70E-06
	>45	3.20E-06
Moderate Permeability Tailings	<15	1.20E-05
	15 - 45	3.30E-06
	>45	9.20E-07
Low Permeability Tailings	<15	2.40E-06
	15 - 45	4.70E-07
	>45	1.50E-07

Figure 8. TSF boundary and tailings types at select times.

Coarse-grained cyclone underflow tailings form the embankment and beach area north of the embankment header line and were assigned the High Permeability tailing type to approximately 61 m of the embankment header line, based on the West transect data.

The interior of the impoundment is predominately composed of the finer textured Low Permeability tailings type, whereas near the impoundment perimeter where spigotting occurs, Moderate Permeability tailings types are found. The transition from Moderate Permeability tailings to Low Permeability tailings was defined as 610 m from the edge of the impoundment based on the East transect percent fines observations and K_{sat} relationships. Similarly, the transition from Moderate to Low Permeability was assumed to be 152 m from the embankment header line on the West transect data. The shorter transition distance from the embankment is due to cyclone overflow from the embankment containing finer textured tailings than the slurry (whole) tailings. Exceptions to the 610 m transition exist near the BOC where Low Permeability tailings were based on observed finer textured tailings and the historic existence of ponding in these areas.

3.5 *Estimated Seepage*

The estimated amount of seepage determined by the water balance model was dominated by seepage from the impoundment (Figure 9). Between 2005 and 2020, predicted seepage from the impoundment was variable and ranged from 125 l/s to 309 l/s. Predicted seepage from the impoundment decreased from 2018 through 2020, relative to 2005 through 2017, due to increased water volume reclaimed to the mill. Future seepage from 2025 through 2028 is predicted to decrease due to projected decreased tailings flow to the TSF and continued tailings consolidation.
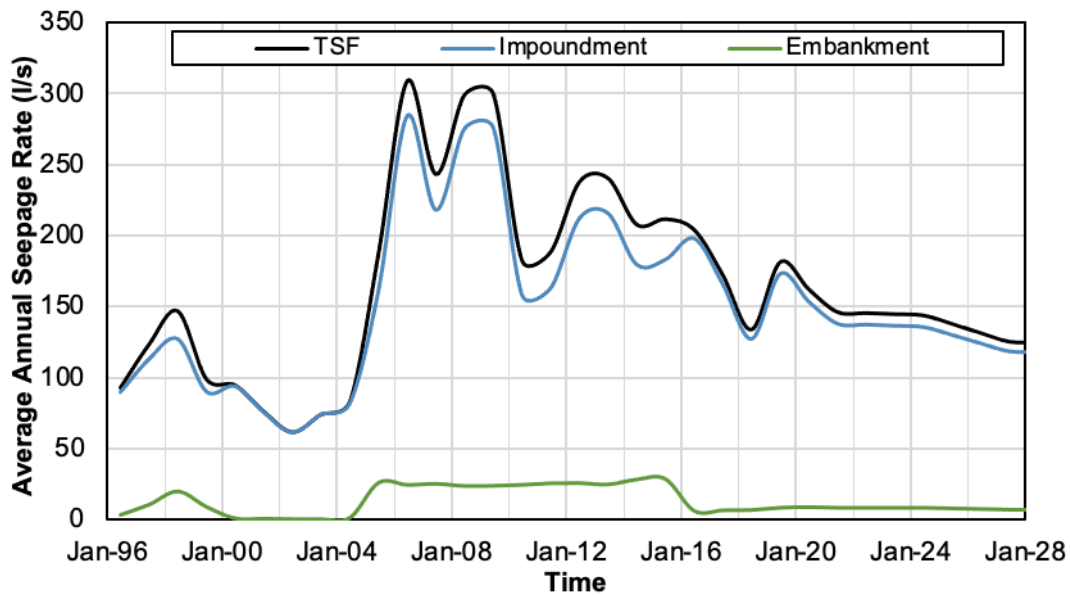
Figure 9. Average annual predicted seepage rate from the TSF, impoundment, and embankment.

Figure 10 shows the predicted distributed seepage from the hydraulic property model during selected timeframes between October-March and April-September. High rates of seepage are predicted to occur from around the perimeter of the impoundment due to the shallow tailings thickness and higher K_{sat} values, low seepage rates are predicted in the center of the impoundment due to the presence of low permeability tailings and consolidation at deeper TSF depths. Over time as the finest particles fill the perimeter areas first and cover the alluvium, and the tailing thickness in these areas become deeper, tailings will continue to consolidate from the overburden pressure causing a reduction in K_{sat} which reduces seepage rates from the interior of the impoundment.

Estimated seepage uncertainty is driven by the largest components of the TSF water balance. The largest inflow component is dominated by water sent to the TSF with the tailings slurry. The largest outflow component, besides seepage, is dominated by impoundment evaporation. Combing these two primary sources of potential uncertainty, the variation in estimated seepage could be 15% lower or 35% higher. Even so, the estimated distributed seepage input into the groundwater model recreated the observed mound growing in groundwater below the TSF.
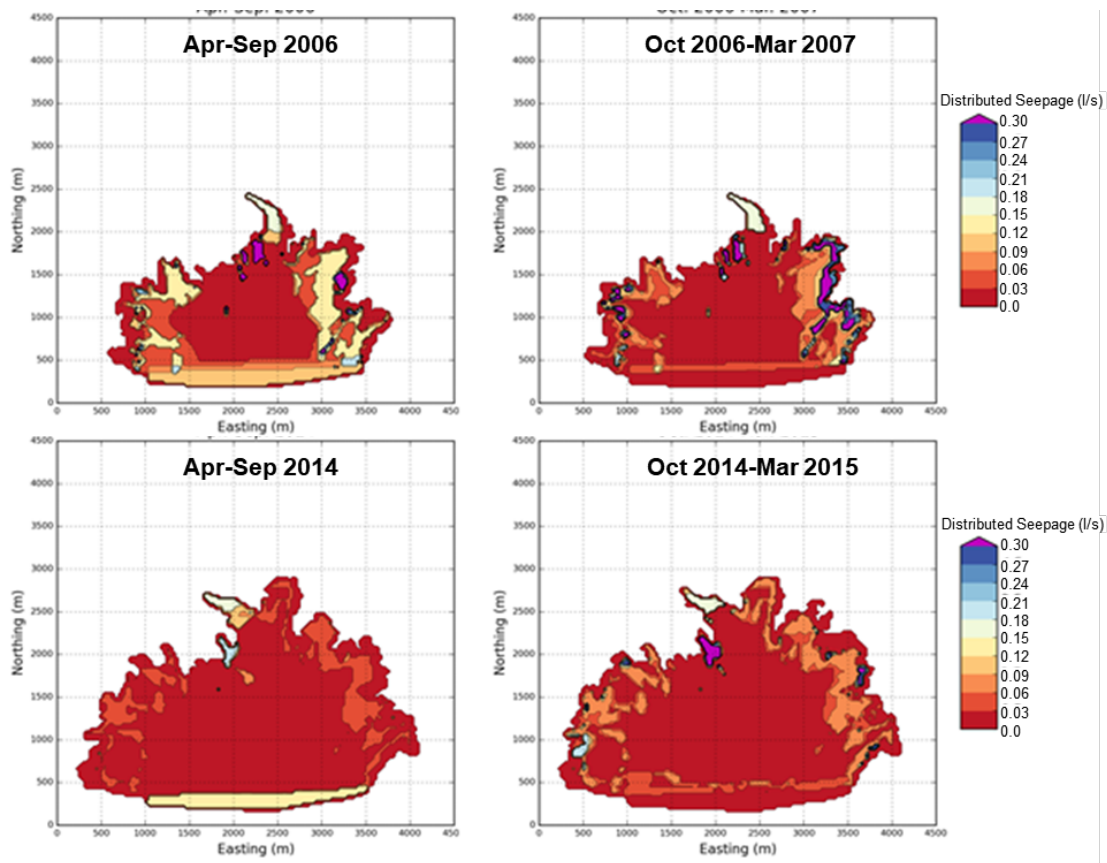
Figure 10. Estimated distributed seepage during selected times.

4 CONCLUSIONS

Conceptual and mathematical water balance models were developed for a large TSF that were constrained by observations and measurement from a combination of field and laboratory characterization data, and desktop analyses. The main objective of this study was to evaluate and quantify the TSF seepage rates that may have occurred during operations, to predict seepage rates that may occur in the future, and the estimated uncertainty. A critical component of the accuracy of past predictions was only allowing infiltration to occur where tailings existed, using the satellite data, and not by making any simplify geometrical assumptions about historical tailings deposition.

A highly detailed water balance model was prepared to estimate all the TSF inflows and outflows with seepage calculated as the difference. A hydraulic property model was also developed to classify tailings material into three different types with specific hydraulic properties. Tailings types were then assigned spatially based the TSF construction over time and distance from the tailings deposition sources. Tailing hydraulic properties were then determined based on the depth of the tailing profile within 30 m by 30 m grids. The hydraulic property model was then used to predict the spatial distribution of seepage across the TSF.

Conclusions regarding the seepage and distributed seepage models are:
- The hydraulic property model was able to distribute seepage to recreate the mound growing in groundwater below the TSF
- Tailing consolidation reduces permeability (seepage) over time as the TSF continues to increase in height, by up to a factor of almost 1,000 times (see Composite #2 in Figure 6), depending on thickness.
- The predicted seepage rates between the water balance and hydraulic property models were in close agreement and indicated that TSF seepage will continue to decrease over time

because the footprint area of the facility will not increase, operational improvements in tailings water management, and increased tailings compaction at depth.

5 REFERENCES

Bouwer, H., J.T. Back, and J.M. Oliver. 1999. Predicting Infiltration and Ground Water Mounds for Artificial Recharge, *J Hydro Eng, ASCE*: 4:350-357.

Bouwer, H. 1966. Rapid Measurement of Air-Entry Value and Hydraulic Conductivity of Soil as Significant Parameters in Flow Systems Analysis, *Water Resour. Res.*: 2:729-738.

Giroud, J.P. and R. Bonaparte. 1989. Leakage through Liners Constructed with Geomembranes – Part I. Geomembrane Liners. *Geotextiles and Geomembranes*: 8:27-67.

Hussen, A.A. and A.W. Warrick. 1993. Alternative analysis of hydraulic data from disc tension infiltrometers. *Water Resour. Res.*: 29:4103–4108.

Keller, J., J. Hendrickx, M. Milczarek, F. Partey, M. Geddis. 2018. High Resolution Estimates of Tailings Facility Evaporation Using Landsat Data. In *Proceedings of Tailings and Mine Waste 2018, Keystone, CO, October 1 - 2, 2018*.

Lee, D.R. 1977. A device for measuring seepage flux in lakes and estuaries. *Limnology and Oceanography*: 22(1):140-147.

Qiu G.Y. and M. Zhao. 2010. Remotely monitoring evaporation rate and soil water status using thermal imaging and "three-temperatures model (3T Model)" under field-scale conditions. *Journal of Environmental Monitoring:* 12(3):716-723.

Wooding, R.A. 1968. Steady infiltration from a shallow circular pond. *Water Resour. Res.*: 4:1259-1273.

United States Department of Agriculture. 1986. Urban hydrology for small watersheds. *Technical Release 55*. Natural Resources Conservation Service.